Phase diagram of two interacting helical states

Raul A. Santos,[1,2] D. B. Gutman,[1] and Sam T. Carr[3]
[1]*Department of Physics, Bar-Ilan University, Ramat Gan 52900, Israel*
[2]*Department of Condensed Matter Physics, Weizmann Institute of Science, Rehovot 76100, Israel*
[3]*School of Physical Sciences, University of Kent, Canterbury CT2 7NH, United Kingdom*
(Received 15 January 2016; revised manuscript received 16 April 2016; published 21 June 2016)

We consider two coupled time-reversal-invariant helical edge modes of the same helicity, such as would occur on two stacked quantum spin Hall insulators. In the presence of interaction, the low-energy physics is described by two collective modes, one corresponding to the total current flowing around the edge and the other one describing relative fluctuations between the two edges. We find that quite generically, the relative mode becomes gapped at low temperatures, but only when tunneling between the two helical modes is nonzero. There are two distinct possibilities for the gapped state depending on the relative size of different interactions. If the intraedge interaction is stronger than the interedge interaction, the state is characterized as a spin-nematic phase. However, in the opposite limit, when the interaction between the helical edge modes is strong compared to the interaction within each mode, a spin-density wave forms, with emergent topological properties. First, the gap protects the conducting phase against localization by weak nonmagnetic impurities; second, the protected phase hosts localized zero modes on the ends of the edge that may be created by sufficiently strong nonmagnetic impurities.

DOI: 10.1103/PhysRevB.93.235436

I. INTRODUCTION

Symmetry-protected topological states of matter are characterized by the invariance of their Hamiltonian under local symmetries. These states are referred to as topological insulators/superconductors. They possess gapless surface modes that are protected by the gap in the bulk of the material, as long as the symmetries are not broken. For noninteracting particles, the topological classification is determined by time-reversal (TR) and particle-hole (PH) symmetry [1,2]. Under this classification, a two-dimensional insulator invariant under TR symmetry can be either trivial or topological. While the bulk conductivity vanishes at zero temperature in both cases, a nontrivial topological insulator (TI) hosts gapless helical edge modes [3,4]. A single helical edge mode consists of a Kramers pair, connected by TR symmetry. The disorder that does not break the TR symmetry cannot scatter between the Kramers partners. Therefore, the system is protected against localization as long as the gap in the bulk exceeds the disorder potential and TR symmetry is preserved. The nontrivial TR topological insulators, also known as quantum spin Hall insulators (QSHIs), have been observed experimentally in certain two-dimensional [5–7] materials with a strong spin orbit. An analogous state occurs in three dimensions [8–10], where the two-dimensional surface is conducting and cannot be localized.

A TR TI in two dimensions is known as a $\mathbb{Z}_2$ topological insulator, meaning that the number of protected topological modes is either zero or one. This means that if one considers a system with two helical edge modes, backscattering between non-Kramers pairs is allowed, leading to Anderson's localization of the edge modes. In this case, the system is a topologically trivial insulator. Whether it is possible to find an individual material exhibiting two (nonprotected) helical modes or not is, as far as we know, an open question. However, such a setup can certainly be engineered by considering a stack of two QSHIs, sufficiently close that the conducting edge modes may both hybridize and interact with each other via the Coulomb interaction (top panel in Fig. 1). A dual stacking to the one proposed here, where a topological insulator is placed parallel to a normal insulator, has been discussed in [11].

The presence of electron-electron interactions can dramatically change the properties even of single QSHIs [12–17]. In particular, as has been shown in Refs. [18,19], the topological protection of a single helical mode in the presence of impurities is removed by sufficiently strong repulsive interactions. The process involves coherent scattering of two interacting electrons off a static impurity, a process allowed by TR symmetry. As a result, the helical state is localized. On the other hand, as shown in Ref. [20], moderate repulsive interaction stabilizes the conducting phase for a TI with a number of edge modes. Clearly these two mechanisms act in opposite directions. In this work, we complete the analysis of [20] and take into account two-particle scattering.

Beyond analyzing the system by considering general terms allowed by symmetry [20–23], we focus on a microscopic model of two helical edge modes, coupled by tunneling, spin-orbit, and electron interaction. In the noninteracting limit, this system is topologically equivalent to a trivial insulator. We show that in the presence of interaction, the system may or may not be topologically trivial depending on the strength of interaction and tunneling amplitude. If the intermode interaction is smaller than the interaction between Kramers pairs, the system remains topologically trivial, with vanishing conductance at zero temperature. In this case, the system is in a spin-nematic phase [24–27]. In the opposite limit, where the intermode interaction is stronger than the interaction within each mode, the system remains conducting. This protection against localization is a direct consequence of the spin gap. By adding strong nonmagnetic impurities, the edge mode splits into unconnected parts, each hosting a pair of localized zero modes on its ends.

This paper is organized as follows. In the first section, we formulate the model. In the second section, we apply the bosonization technique and analyze the low-temperature fixed point using the renormalization-group (RG) approach. In the

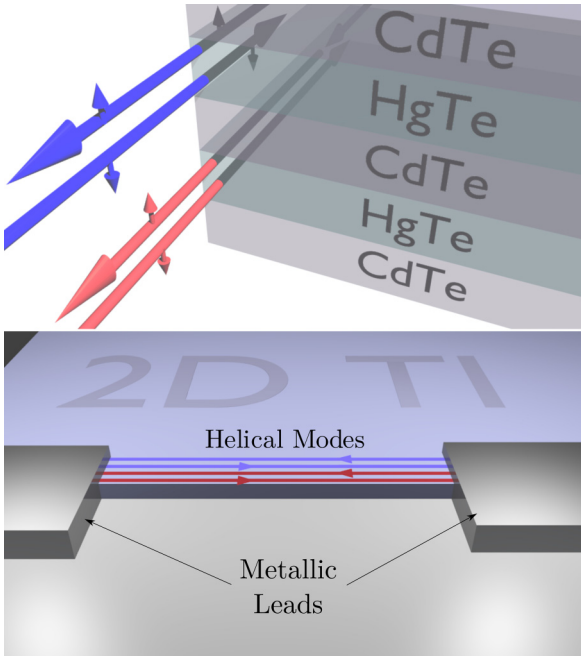

FIG. 1. Top: A stack of quantum wells, each realizing a helical edge mode, becomes effectively a topological insulator with two helical edge modes. Bottom: Experimental setup to measure the conductance (see text).

third section, we study the stability of the conducting phase against a single impurity and random disorder. We summarize and discuss our results in the Conclusion.

II. TWO COUPLED HELICAL MODES

A. Motivation

It is well known [1] that in the case of vanishing interactions, a putative TR TI with two helical edge modes (each of them composed of a right mover and a left mover with opposite spins projections), the topological protection, which is the hallmark of the TR TI with a single helical mode, is no longer present. This implies that in a real material, edge roughness and/or a local spin orbit can localize the pair of helical edge modes, causing the conductance in the system to tend to zero at vanishing temperatures. In this section, we introduce the minimal effective theory, valid at low temperatures, that contains all the ingredients to analyze the effects of interactions in an edge of a TI supporting two helical modes. Although no such system has been found experimentally yet, such a system is the natural generalization of a TI with a single helical edge mode, and it is a candidate for the description of the edge in a heterostructure (Fig. 1, top). Similar setups were considered in the pioneering works of Wu, Bernevig, and Zhang [21] and Tanaka and Nagaosa [22]. The noteworthy aspect of our paper stems from taking into account the generic spin orbit, which violates the conservation of the z component of the spin. We thus keep the simplest most relevant term, in a renormalization-group sense, generated by such interaction. In this regard, a local interaction term is it known to capture the basic physics [25]. The important effects of disorder are considered in Sec. IV.

B. The model

We consider two interacting helical modes. Each one is formed at the edge of two-dimensional TR invariant topological insulators that are placed one next to the other; see Fig. 1. The Hamiltonian of the clean system (disorder or impurities will be added in Sec. IV) consists of four different parts,

$$H = H_{\rm kin} + H_{\rm tun} + H_{\rm SO} + H_{\rm int}. \tag{1}$$

Here $H_{\rm kin}$ is the kinetic energy,

$$H_{\rm kin} = \sum_{k,\sigma,a} \epsilon_{\sigma,a}(k) c^\dagger_{\sigma,a}(k) c_{\sigma,a}(k), \tag{2}$$

where $c^\dagger_{\sigma,a}(k)$ creates a fermion in a helical mode ($a = 1,2$) with a given spin ($\sigma = \uparrow, \downarrow$) and momentum k; $\epsilon_{\sigma,a}(k)$ is the dispersion relation of the noninteracting mode. The helicity comes from the relationship between spin σ and the dispersion—roughly speaking, spin up will correspond to a right-moving mode, while spin down will be a left-moving mode; this will be fully discussed below.

The tunneling between the two modes is described by

$$H_{\rm tun} = -t_\perp \sum_{k,\sigma,a} c^\dagger_{\sigma,a}(k) c_{\sigma,\bar{a}}(k), \tag{3}$$

where we introduced the notation $\bar{1} = 2, \bar{2} = 1$.

In a TI, spin-orbit coupling creates a band inversion in the topological phase, which is responsible for the appearance of edge modes in the first place. On top of this spin-orbit coupling, which is present in the bulk of the system, the very presence of a boundary in a generic system will induce a different spin-orbit coupling potential near the edges, which could be caused by an interplay between the Rashba and the Dresselhaus coupling in crystals without inversion symmetry. As part of the model, we consider spin-orbit coupling on the edge (which breaks S_z conservation). While many previous works did this at a phenomenological level (as TRS does not imply unbroken S_z symmetry), we expand on a model originally proposed for a single edge by Schmidt *et al.* [18]. In this model, the spin-orbit coupling $H_{\rm SO}$ is explicitly incorporated into the noninteracting part of the model, as this is the physical process that leads to broken spin-rotation symmetry. In the low-energy description, the simplest coupling $H_{\rm SO}$ has the generic form

$$H_{\rm SO} = \alpha_{\rm SO} \sum_{k,\sigma,\sigma',a} k c^\dagger_{\sigma,a}(k) (\sigma^x)_{\sigma,\sigma'} c_{\sigma',a}(k), \tag{4}$$

with σ^x being the corresponding Pauli matrix.

Finally, the interaction between electrons is modeled by

$$H_{\rm int} = U_0 \sum_{x,a} n_a(x) n_a(x) + 2U \sum_x n_1(x) n_2(x), \tag{5}$$

where the Coulomb interaction is replaced by a local Hubbard term, which contains the relevant physics at low energies. Here U_0 and U stand for interaction constants within the same mode

and between different modes consequently. Under generic conditions, these two constants are different ($U_0 \neq U$). The fermion densities are

$$n_a(x) = c^\dagger_{\uparrow,a}(x)c_{\uparrow,a}(x) + c^\dagger_{\downarrow,a}(x)c_{\downarrow,a}(x), \tag{6}$$

where, as usual, $c_{\sigma,a}(x) = \sum_k e^{ikx}c_{\sigma,a}(k)$.

Throughout this work, we will use units where $\hbar = 1$ and a_0 is the short-distance cutoff for the field theory. This may be thought of as an effective lattice spacing for the helical modes; however, in a full theory of the entire two-dimensional setup of the QSHI, it is more closely related to the inverse of the bulk gap. In either case, it is a nonuniversal constant in the field theory that sets the overall energy scale.

C. Diagonalization of the noninteracting Hamiltonian

In a TR invariant system, the dispersion relation must satisfy the constraint

$$\epsilon_{\sigma,a}(k) = \epsilon_{\bar{\sigma},a}(-k). \tag{7}$$

The simplest dispersion relations describing gapless modes are $\epsilon_{\uparrow,a}(k) = v_F k$ and $\epsilon_{\downarrow,a}(k) = -v_F k$. Here we assume that the Fermi velocity of the noninteracting helical modes is the same. Introducing the vector of fermionic fields,

$$\boldsymbol{c}^\dagger(k) = (c^\dagger_{\uparrow,1}(k), c^\dagger_{\downarrow,1}(k), c^\dagger_{\uparrow,2}(k), c^\dagger_{\downarrow,2}(k)), \tag{8}$$

the noninteracting part of the Hamiltonian $H_0 = H_{\rm kin} + H_{\rm tun} + H_{\rm SO}$ becomes

$$H_0 = \sum_k \boldsymbol{c}^\dagger(k)h_0(k)\boldsymbol{c}(k), \tag{9}$$

with $h_0(k)$ the Hermitian matrix,

$$h_0 = \begin{bmatrix} v_F k & \alpha_{\rm SO} k & -t_\perp & 0 \\ \alpha_{\rm SO} k & -v_F k & 0 & -t_\perp \\ -t_\perp & 0 & v_F k & \alpha_{\rm SO} k \\ 0 & -t_\perp & \alpha_{\rm SO} k & -v_F k \end{bmatrix} \tag{10}$$

$$= \delta_{aa'}\left(v_F \sigma^z_{\sigma\sigma'} + \alpha_{\rm SO}\sigma^x_{\sigma\sigma'}\right)k - t_\perp \tau^x_{aa'}\delta_{\sigma\sigma'}. \tag{11}$$

Here $\sigma^{x,y,z}, \tau^{x,y,z}$ are the corresponding Pauli matrices in spin and mode space, respectively. Using (11) we find that $h_0(k)$ is diagonalized by a unitary transformation B, such that $h_0(k) = B^\dagger D(k) B$, with

$$B = \frac{1}{\sqrt{2}}\begin{bmatrix} \cos\beta & \sin\beta & \cos\beta & \sin\beta \\ -\sin\beta & \cos\beta & -\sin\beta & \cos\beta \\ \cos\beta & \sin\beta & -\cos\beta & -\sin\beta \\ -\sin\beta & \cos\beta & \sin\beta & -\cos\beta \end{bmatrix} \tag{12}$$

$$= \frac{\left(\tau^z_{aa'} + \tau^x_{aa'}\right)}{\sqrt{2}}\left(e^{i\beta\sigma^y}\right)_{\sigma\sigma'}, \tag{13}$$

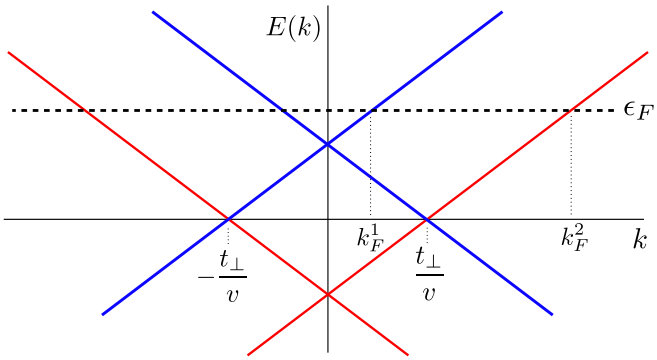

FIG. 2. Single-particle energy spectrum. Kramers pairs are depicted by the same color.

and $\beta = \frac{1}{2}\tan^{-1}(\frac{\alpha_{\rm SO}}{v_F})$. We therefore pass to the new basis

$$\boldsymbol{\psi}(k) = B\boldsymbol{c}(k), \quad \boldsymbol{\psi}^\dagger = (\psi^\dagger_{+,1}, \psi^\dagger_{-,1}, \psi^\dagger_{+,2}, \psi^\dagger_{-,2}), \tag{14}$$

where the single-particle Hamiltonian (9) is diagonal,

$$H_0 = \sum_k \boldsymbol{\psi}^\dagger(k)D(k)\boldsymbol{\psi}(k). \tag{15}$$

The eigenenergies are given by $D(k) = {\rm diag}(vk - t_\perp, -vk - t_\perp, vk + t_\perp, -vk + t_\perp)$, where $v = \sqrt{v_F^2 + \alpha_{\rm SO}^2}$ is the renormalized Fermi velocity. These dispersion relations are shown in Fig. 2.

It is worth emphasizing that while in the original basis $c_{\sigma,a}$, σ corresponded to the physical spin and a to the helical edge in question, in the new basis $\psi_{\sigma,a}$, σ corresponds to helicity and a to the band index. Thus the transformation matrix (12) encodes the relationship between spin and helicity that will be crucially important when potential disorder is added in Sec. IV.

D. Interacting Hamiltonian in a rotated basis

In the new basis $\boldsymbol{\psi}$, the interaction part of the Hamiltonian becomes

$$H_{\rm int} = \sum_{x,\sigma\sigma' aa'}\Bigg(U_+\psi^\dagger_{\sigma a}(x)\psi_{\sigma a}(x)\psi^\dagger_{\sigma' a'}(x)\psi_{\sigma' a'}(x) + U_-\sum_{a_1,a_2}\psi^\dagger_{\sigma a}(x)(\tau^x)_{aa_1}\psi_{\sigma a_1}(x) \times \psi^\dagger_{\sigma' a'}(x)(\tau^x)_{a'a_2}\psi_{\sigma' a_2}(x)\Bigg),$$

with $U_\pm = (U_0 \pm U)/2$. In the continuum limit, it is convenient to rewrite the field operators in terms of slow modes near each Fermi point [25,27,28]:

$$\psi_{+,1}(x) \to R_1(x)e^{ik_F^1 x}, \quad \psi_{-,1}(x) \to L_1(x)e^{-ik_F^1 x},$$
$$\psi_{+,2}(x) \to R_2(x)e^{ik_F^2 x}, \quad \psi_{-,2}(x) \to L_2(x)e^{-ik_F^2 x}.$$

Here the Fermi momenta $k_F^{1,2}$ are given by $(\epsilon_F \pm t_\perp)/v$. The noninteracting Hamiltonian can be written in terms of the slow

modes in a standard way,

$$H_0 = -iv\int dx \sum_a (R_a^\dagger \partial_x R_a - L_a^\dagger \partial_x L_a). \tag{16}$$

The interaction Hamiltonian acquires the form

$$H_{\rm int} = \frac{U_+}{2}\int dx \sum_a (R_a^\dagger R_a + L_a^\dagger L_a)^2 \tag{17a}$$

$$+ U_- \int dx (R_1^\dagger R_1 R_2^\dagger R_2 + L_1^\dagger L_1 L_2^\dagger L_2) \tag{17b}$$

$$+ U_- \int dx (R_1^\dagger R_2 L_1^\dagger L_2 + L_2^\dagger L_1 R_2^\dagger R_1) \tag{17c}$$

$$+ U_- \int dx (R_1^\dagger R_2 L_2^\dagger L_1 e^{2i\Delta k_F x} + \text{H.c.}), \tag{17d}$$

with $U_\pm = U_0 \pm U$ and $\Delta k_F = k_F^1 - k_F^2 = 2t_\perp/v$.

III. BOSONIZATION AND RG ANALYSIS

To account for the effects of the interaction, it is natural to proceed to the bosonic description of fermionic fields. The fermionic fields are represented by the vertex operators

$$R_i = \frac{\kappa_i}{\sqrt{2\pi a_0}} e^{i\sqrt{4\pi}\phi_i^R}, \quad L_i = \frac{\kappa_i}{\sqrt{2\pi a_0}} e^{-i\sqrt{4\pi}\phi_i^L}. \tag{18}$$

The bosonic fields satisfy the equal-time commutation relations

$$\left[\phi_i^R(x), \phi_j^L(x)\right] = \frac{i}{4}\delta_{ij} \quad \text{(same point)}, \tag{19}$$

$$\left[\phi_i^\eta(x), \phi_j^{\eta'}(y)\right] = \frac{i}{4}\eta\delta_{ij}\delta_{\eta\eta'}\text{sgn}(x-y). \tag{20}$$

After bosonization [25,27,28], the noninteracting part of the Hamiltonian (16) combines with (17a) and (17b) into the quadratic bosonic Hamiltonian

$$H_{\rm quad} = v\int dx \sum_a \left[\left(\partial_x \phi_a^R\right)^2 + \left(\partial_x \phi_a^L\right)^2\right] + g\int dx \sum_a \left(\partial_x \phi_a^R + \partial_x \phi_a^L\right)^2 + g'\int dx \left(\partial_x \phi_1^R \partial_x \phi_2^R + \partial_x \phi_1^L \partial_x \phi_2^L\right). \tag{21}$$

Here $g = (U_0 + U)a_0/2\pi$, $g' = (U_0 - U)a_0/2\pi$, and a_0 is the lattice constant. The interaction Hamiltonian also generates the backscattering terms

$$H_{\rm bs} = -\frac{g'}{\pi a_0^2}\int dx \left(e^{i\sqrt{4\pi}(\phi_1^L - \phi_1^R - \phi_2^L + \phi_2^R)} + \text{H.c.}\right) + \frac{g'}{\pi a_0^2}\int dx \left(e^{i\sqrt{4\pi}(\phi_1^L + \phi_1^R - \phi_2^L - \phi_2^R)} e^{i\Delta x} + \text{H.c.}\right). \tag{22}$$

In terms of the new bosonic fields,

$$\begin{bmatrix}\varphi_+\\ \theta_+\\ \varphi_-\\ \theta_-\end{bmatrix} = \frac{1}{\sqrt{2}}\begin{bmatrix}1 & 1 & 1 & 1\\ 1 & -1 & 1 & -1\\ 1 & 1 & -1 & -1\\ 1 & -1 & -1 & 1\end{bmatrix}\begin{bmatrix}\phi_1^L\\ \phi_1^R\\ \phi_2^L\\ \phi_2^R\end{bmatrix}, \tag{23}$$

the full Hamiltonian (16)–(17d) splits into two commuting parts $H = H_+ + H_-$. The Hamiltonian H_+ is given by

$$H_+ = \frac{u_+}{2}\int dx \left[\frac{(\partial_x \varphi_+)^2}{K} + (\partial_x \theta_+)^2 K\right], \tag{24}$$

where $u_+ = \sqrt{(v+g')(v+g'+4g)}$ and the Luttinger parameter is $K = \sqrt{\frac{v+g'}{v+g'+4g}}$. The second part of the Hamiltonian, H_-,

$$H_- = \frac{u_-}{2}\int dx [(\partial_x \varphi_-)^2 + (\partial_x \theta_-)^2] - \frac{g'}{\pi a_0^2}\int dx (\cos(\sqrt{8\pi}\theta_-) - \cos(\sqrt{8\pi}\varphi_- + 2\Delta k_F x)), \tag{25}$$

with $u_- = v - g'$. Note that due to the helical nature of the fermionic modes, the bare Luttinger parameter K_- of the Hamiltonian H_- equals unity. The RG equations depend on the ratio between the running scale to the tunneling amplitude.

For energies above $t_\perp$, one can ignore the oscillating part $2\Delta k_F x$ in the second cosine, and the model is equivalent to the bosonized form of the XYZ chain, naturally tuned to be on a Z_4 plane in the phase diagram (see, e.g., Ref. [25]). The RG equations are

$$\frac{\partial K_-}{\partial \ell} = 0, \quad \frac{\partial \tilde{g}}{\partial \ell} = 0. \tag{26}$$

Here $\ell = \ln \Lambda_0/\Lambda$ (with Λ being a running energy scale), and $\tilde{g} = g'/u_- = a_0(U_0 - U)/2\pi u_-$. Clearly, neither the Luttinger parameter nor the amplitude of the cosines renormalizes in this regime. The Luttinger parameter therefore remains unity and the theory remain gapless, as shown by refermionization back to the original fermionic degrees of freedom.

However, below the energy scale $t_\perp$, the presence of the oscillations $2\Delta k_F x$ in the second cosine term in (25) becomes important, and therefore averaged over long energy scales this entire cosine term can be neglected in the RG flow at these energy scales [29]. One is then left with the well-known sine-Gordon model; the RG equations in this case read [25,28]

$$\frac{\partial K_-}{\partial \ell} = -\tilde{g}^2, \quad \frac{\partial \tilde{g}}{\partial \ell} = (1 - K_-)\tilde{g}. \tag{27}$$

We see that both K_- and $\tilde{g}$ always flow to strong coupling as the energy scale is reduced ($\ell \to \infty$). Therefore, the term $\cos(\sqrt{8\pi}\theta_-)$ opens a gap in the mode described by ϕ_-, θ_-. In this situation, the system flows to one of two strong-coupling fixed points depending on the sign of g'. We note, however, that the other mode, ϕ_+, θ_+, always remains gapless in the absence of any umklapp scattering.

At this point, it is also worth emphasizing the importance of interchain hopping $t_\perp \neq 0$ in the above result. In its absence, $t_\perp = 0$, one would never enter the second range of RG flow, and Eq. (26) would be valid until arbitrarily low temperatures. Thus the interchain hopping is necessary for a strong-coupling phase to occur (for weak interactions). We now proceed to characterize the two strong-coupling phases by looking at potential local order parameters. As one of the modes remains gapless, these local order parameters are never nonzero in the thermodynamic limit, rather the phase is identified as the order parameter with the slowest decaying correlations; see, e.g., Refs. [30,31].

A. Intramode interaction stronger than intermode interaction ($g' > 0$)

For positive g', the minimum of $-g'\cos(\sqrt{8\pi}\theta_-)$ takes place at $\theta_- = \sqrt{\frac{\pi}{2}}n$ with $n \in \mathbb{Z}$. In this case, the order parameter [with $\bar{k}_F = (k_F^1 + k_F^2)/2 \equiv \epsilon_F/v$]

$$\begin{aligned} O_I &= i(e^{2i\bar{k}_F x}\psi^\dagger_{+,1}\psi_{-,2} + e^{-2i\bar{k}_F x}\psi^\dagger_{-,1}\psi_{+,2} - \text{H.c.}) \\ &= \frac{1}{\pi a_0}\left[\cos\sqrt{4\pi}\left(\phi_1^R + \phi_2^L\right) + \cos\sqrt{4\pi}\left(\phi_2^R + \phi_1^L\right)\right] \\ &= \frac{2}{\pi a_0}\cos(\sqrt{2\pi}\theta_-)\cos(\sqrt{2\pi}\varphi_+) \end{aligned} \tag{28}$$

becomes dominant as $\langle\cos\sqrt{2\pi}\theta_-\rangle \neq 0$. In terms of the original helical fermions $c_{\sigma,a}$, this order parameter reads

$$\begin{aligned} O_I = \cos 2\bar{k}_F x \sum_{\sigma\sigma' aa'} c^\dagger_{\sigma a}(\tau^y)_{aa'}[\cos 2\beta\sigma^x - \sin 2\beta\sigma^z]_{\sigma\sigma'}c_{\sigma' a'} \\ - \sin 2\bar{k}_F x \sum_{\sigma\sigma' aa'} c^\dagger_{\sigma a}(\tau^y)_{aa'}(\sigma^y)_{\sigma\sigma'}c_{\sigma' a'}. \end{aligned} \tag{29}$$

To understand the structure of this order parameter, we can rotate the spin-quantization axis in the xz plane by defining the rotated fermionic operators $\tilde{c}_{\sigma,a} = \sum_{\sigma'}(e^{i(\beta-\pi/4)\sigma^y})_{\sigma\sigma'}c_{\sigma',a}$. In this basis,

$$O_I = \sum_{\sigma\sigma' aa'} \tilde{c}^\dagger_{\sigma a}(\tau^y)_{aa'}[\cos 2\bar{k}_F x\ \sigma^z - \sin 2\bar{k}_F x\ \sigma^y]_{\sigma\sigma'}\tilde{c}_{\sigma' a'}. \tag{30}$$

The τ^y in this order parameter means that a pattern of currents is flowing between the two spin edges. The presence of σ^x and σ^y (rather than σ^0) means that these are spin currents; the spatially dependent part in brackets describes a spiral for the axis of quantization of these currents.

We should be very clear here that this order parameter is not proportional to a spin density, but rather a *spin current* [24–27]. Such a state goes by a number of different names, such as spin-nematic [24] or triplet D-density wave [26]. The present order parameter is somewhat more intricate than those cited, as the quantization axis for the current is spatially varying in a spiral. Nevertheless, we will concisely refer to this phase as spin nematic, after Ref. [24], where this type of order parameter was first considered.

B. Intermode interaction stronger than intramode interaction ($g' < 0$)

For negative g', the minimum of $-g'\cos(\sqrt{8\pi}\theta_-)$ occurs at $\theta_- = \sqrt{\frac{\pi}{2}}(n + \frac{1}{2})$ with $n \in \mathbb{Z}$. In this case, the order parameter

$$\begin{aligned} O_{II} &= e^{2i\bar{k}_F x}(\psi^\dagger_{+,1}\psi_{-,2} + \psi^\dagger_{+,2}\psi_{-,1}) + \text{H.c.} \\ &= \frac{1}{\pi a_0}\left[\sin\sqrt{4\pi}\left(\phi_1^R + \phi_2^L\right) - \sin\sqrt{4\pi}\left(\phi_2^R + \phi_1^L\right)\right] \\ &= \frac{2}{\pi a_0}\sin(\sqrt{2\pi}\theta_-)\cos(\sqrt{2\pi}\varphi_+) \end{aligned} \tag{31}$$

becomes dominant as $\langle\sin\sqrt{2\pi}\theta_-\rangle \neq 0$. In terms of the original helical fermions $c_{\sigma,a}$, this order parameter reads

$$\begin{aligned} O_{II} = \cos 2\bar{k}_F x \sum_{\sigma\sigma' aa'} c^\dagger_{\sigma a}(\tau^z)_{aa'}[\cos 2\beta\sigma^x - \sin 2\beta\sigma^z]_{\sigma\sigma'}c_{\sigma' a'} \\ - \sin 2\bar{k}_F x \sum_{\sigma\sigma' aa'} c^\dagger_{\sigma a}(\tau^z)_{aa'}(\sigma^y)_{\sigma\sigma'}c_{\sigma',a'}. \end{aligned} \tag{32}$$

Again, performing a rotation in the spin basis $\tilde{c}_{\sigma,a} = \sum_{\sigma'}(e^{i(\beta-\pi/4)\sigma^y})_{\sigma\sigma'}c_{\sigma',a}$, the order parameter can be written in the familiar form

$$O_{II} = \sum_{\sigma\sigma' aa'} \tilde{c}^\dagger_{\sigma a}(\tau^z)_{aa'}[\cos 2\bar{k}_F x\ \sigma_z - \sin 2\bar{k}_F x\ \sigma^y]_{\sigma\sigma'}\tilde{c}_{\sigma',a'}. \tag{33}$$

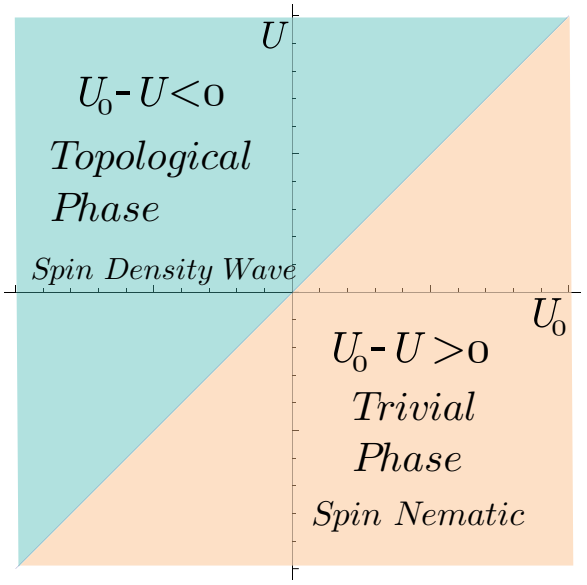

FIG. 3. Dominant order parameter for two interacting helical modes, for strong tunneling. Here $g' = (U_0 - U)/2\pi$, where U_0 is the interaction strength within a helical mode, whereas U is the mutual interaction between the modes. Above the diagonal, the dominant correlations are of the spin-density-wave type, while below the diagonal, the dominant correlations are of the spin-nematic type. H_- remain gapless along the diagonal $U_0 = U$.

The only difference between this order parameter and that in Eq. (30) is the replacement of τ^y with τ^z. This means that instead of spin currents, one has a pattern of spins, with the two different helical edges antiferromagnetically connected. The state is therefore a spin density wave (SDW). Rather like the spin nematic state previously considered, this SDW is not simple as the axis of quantization slowly rotates in a spiral, leading to an interwoven helical arrangement of the spins between the two edges. The important physics we discuss, however, comes not from the precise spatial structure of the order parameter, but rather from the fact that it is proportional to spin density rather than spin current; we will therefore simply refer to this state as a SDW.

Putting these two results together, the entire phase diagram of the problem in the absence of disorder is depicted in Fig. 3.

IV. DISORDER

We now consider the response of the coupled edge system to backscattering; first we consider the case of single impurities, and then we go on to look at random disorder. We follow closely methods previously developed for ordinary (nonhelical) two-leg ladders [30–32]. Rather similarly to two-leg ladders, we will find that one of the strong-coupling phases is particularly susceptible to localization by disorder, while in the other phase the system remains a ballistic conductor, even when disorder is added (rather like the original helical edges before they were coupled).

We then go on to show that the conducting phase actually has emergent topological properties, namely zero-energy boundary states, before discussing experimental signatures of the results of the calculations in this section.

A. Single impurity

For isolated helical modes, nonmagnetic impurities cannot localize the metallic state for moderate interaction. In the noninteracting limit, the backscattering between counterpropagating modes is not allowed by the Kramers theorem. If interaction within a helical mode is strong ($K < 1/4$), the single impurity is a relevant perturbation. For the random disorder, the localization occurs at $K < 3/8$ [18,19]. Here we analyze the fate of the conducting state when two helical modes are present. The presence of a nonmagnetic impurity at $x = 0$ generates the scattering processes [here $c_{\sigma,a} = c_{\sigma,a}(x = 0)$]

$$H^{\parallel}_{\rm imp} = \sum_{\sigma,a} \mu^{\parallel}_a c^\dagger_{\sigma,a} c_{\sigma,a}, \tag{34}$$

$$H^{\perp}_{\rm imp} = \mu^{\perp}(c^\dagger_{\uparrow,1}c_{\uparrow,2} + c^\dagger_{\downarrow,2}c_{\downarrow,1}) + \text{H.c.} \tag{35}$$

In general, for a TR invariant impurity potential, $\mu^{\parallel}_{1,2}$ are real numbers while $\mu^{\perp} = \mu^{\perp}_{\rm Re} + i\mu^{\perp}_{\rm Im}$ can be a complex number. A finite imaginary part of $\mu^{\perp}$ implies the breaking of inversion symmetry by the disorder potential. Let us note that inversion symmetry is broken already at the level of the single-particle Hamiltonian (1), as the helical modes break explicitly the right-left symmetry due to their different spin projections. Writing the real and imaginary parts of $\mu^{\perp}$, the impurity scattering processes $H^{\perp}_{\rm imp}$ read

$$H^{\perp}_{\rm imp} = \mu^{\perp}_{\rm Re} \sum_{\sigma\sigma' aa'} c^\dagger_{\sigma a}(\tau^x)_{aa'}\delta_{\sigma\sigma'}c_{\sigma' a'} - \mu^{\perp}_{\rm Im} \sum_{\sigma\sigma' aa'} c^\dagger_{\sigma a}(\tau^y)_{aa'}(\sigma^z)_{\sigma\sigma'}c_{\sigma' a'}. \tag{36}$$

In the basis (14), the forward part of the impurity scattering is given by

$$H^{\rm f}_{\rm imp} = \sum_{\sigma,a} \mu_a \psi^\dagger_{\sigma,a}\psi_{\sigma,a} + \mu^{\parallel}_- \sum_{\sigma}(\psi^\dagger_{\sigma,1}\psi_{\sigma,2} + \text{H.c.}) + \mu^{\perp}_{\rm Im}\cos 2\beta \sum_{\sigma\sigma' aa'} \psi^\dagger_{\sigma a}(\tau^y)_{aa'}(\sigma^z)_{\sigma\sigma'}\psi_{\sigma' a'}, \tag{37}$$

with $\mu_{1,2} = \frac{\mu^{\parallel}_1+\mu^{\parallel}_2}{2} \pm \mu^{\perp}_{\rm Re}$ and $\mu^{\parallel}_- = \frac{\mu^{\parallel}_1-\mu^{\parallel}_2}{2}$. The backscattering terms are accounted by

$$H^{b}_{\rm imp} = \mu^{\perp}_{\rm Im}\sin 2\beta \sum_{\sigma\sigma' aa'} \psi^\dagger_{\sigma a}(\tau^y)_{aa'}(\sigma^x)_{\sigma\sigma'}\psi_{\sigma' a'}.$$

The forward processes do not play any role in the Anderson localization, and therefore they will be neglected. One is left with the backscattering term

$$H^{\rm b}_{\rm imp} = \mu^{\perp}_{\rm Im}\sin 2\beta \sum_{\sigma\sigma' aa'} \psi^\dagger_{\sigma a}(\tau^y)_{aa'}(\sigma^x)_{\sigma\sigma'}\psi_{\sigma' a'}. \tag{38}$$

After bosonization, this term reads

$$H^{\rm b}_{\rm imp} = -i\mu^{\perp}_{\rm Im}\sin 2\beta[R^\dagger_1 L_2 + L^\dagger_1 R_2 - R^\dagger_2 L_1 - L^\dagger_2 R_1] = -\frac{2\mu^{\perp}_{\rm Im}}{\pi a_0}\sin 2\beta\cos(\sqrt{2\pi}\theta_-)\cos(\sqrt{2\pi}\varphi_+). \tag{39}$$

For $g' > 0$ when the system is in the spin-nematic phase, the expectation value of $\cos\sqrt{2\pi}\theta_-$ is finite. This implies that the scattering operator is determined by $\cos\sqrt{2\pi}\varphi_+$. Under RG its scaling dimension is $K/2 < 1$. Therefore, it is a relevant perturbation, making the system an insulator. In the opposite case, for $g' < 0$ in the spin-density wave state, the expectation value of $\cos\sqrt{2\pi}\theta_-$ is zero and the backscattering operator is always irrelevant. Therefore, the system remains conducting.

B. Random disorder

We now turn to another limit of disorder, where one considers many weak nonmagnetic impurities. In this case, the previous analysis should be modified. The disorder is accounted for by $H_{\rm dis} = H^{\parallel}_{\rm dis} + H^{\perp}_{\rm dis}$ with

$$H^{\parallel}_{\rm dis} = \int dx \sum_{\sigma,a} \mathcal{U}^{\parallel}_a(x) c^\dagger_{\sigma,a}(x)c_{\sigma,a}(x),$$

$$H^{\perp}_{\rm dis} = \int dx\, \mathcal{U}^{\perp}(x)[c^\dagger_{\uparrow,1}(x)c_{\uparrow,2}(x) + c^\dagger_{\downarrow,2}(x)c_{\downarrow,1}(x)] + \text{H.c.} \tag{40}$$

The components of random potential $\mathcal{U}^{\perp}(x')$ are given by

$$\mathcal{U}^{\perp}(x) = \int dy\, U(x,y)\chi_1(y)\chi^*_2(y-d), \tag{41}$$

$$\mathcal{U}^{\parallel}_a(x) = \int dy\, U(x,y)\chi_a(y)\chi^*_a(y), \tag{42}$$

where $U(x,y)$ is the two-dimensional random potential generated by the impurities. The wave function of the helical mode a in the direction perpendicular to the motion is $\chi_a(y)$. The function $\chi(y)$ is peaked around zero, as the helical edge modes are quasi-one-dimensional. The separation d between the modes is assumed to be constant.

We assume that the disorder at different points is uncorrelated, i.e., $\overline{\mathcal{U}_a^{\parallel}(x)\mathcal{U}_b^{\parallel}(x')} = \delta_{ab}\delta(x-x')$ and $\overline{[\mathcal{U}^{\perp}(x)]^*\mathcal{U}^{\perp}(x')} = D\delta(x-x')$. As in the case of a single impurity, the disordered Hamiltonian $H_{\rm dis}^{\parallel}$ in the single-particle diagonal basis ψ contains just forward scattering terms, which do not localize the system. We concentrate in $H_{\rm dis}^{\perp}$, which in the ψ basis becomes

$$H_{\rm dis}^{\perp} = \int dx \sum_{\sigma\sigma' aa'} (\mathcal{U}_{\rm Re}^{\perp}(x)\psi_{\sigma a}^{\dagger}(x)(\tau^z)_{aa'}\delta_{\sigma\sigma'}\psi_{\sigma a'}(x) + \mathcal{U}_{\rm Im}^{\perp}(x)\psi_{\sigma a}^{\dagger}(x)(\tau^y)_{aa'}[\vec{n}(\beta)\cdot\vec{\sigma}]_{\sigma\sigma'}\psi_{\sigma' a'}(x)), \quad (43)$$

where $\mathcal{U}_{\rm Re\,(Im)}^{\perp}$ is the real (imaginary) part of the disorder potential $\mathcal{U}^{\perp}$. The vector $\vec{n}$ is unitary and explicitly given by $\vec{n}(\beta) = (\sin 2\beta, 0, \cos 2\beta)$. Focusing on the backscattering terms, we have

$$H_{\rm dis}^{\rm b} = \frac{1}{2}\int dx \sum_{\sigma\sigma' aa'} \eta(x,\beta)\psi_{\sigma a}^{\dagger}(\tau^y)_{aa'}(\sigma^x)_{\sigma\sigma'}\psi_{\sigma' a'}, \quad (44)$$

with $\eta(x,\beta) = 2\mathcal{U}_{\rm Im}^{\perp}(x)\sin 2\beta$. Under bosonization, this term becomes

$$H_{\rm imp}^{\rm b} = -\frac{i}{2}\int dx\, \eta(x,\beta)[(R_1^{\dagger}L_2 - R_2^{\dagger}L_1)e^{-i\delta x} - \text{H.c.}] = -\frac{1}{\pi a_0}\int dx\, \eta(x,\beta)\cos(\sqrt{2\pi}\theta_-)\cos(\sqrt{2\pi}\varphi_+ + \delta x), \quad (45)$$

with $\delta = 2\epsilon_F/v$. Averaging over disorder, one finds the replicated action that is generated by the backscattering term (45),

$$S_{\rm imp}^{b,\rm av} = \frac{D}{(\pi a_0)^2}\sum_{\alpha\beta}\int dx\, d\tau_1 d\tau_2 \cos(\sqrt{2\pi}\theta_-^{\alpha})\cos(\sqrt{2\pi}\varphi_+^{\alpha}) \times \cos(\sqrt{2\pi}\theta_-^{\beta})\cos(\sqrt{2\pi}\varphi_+^{\beta}). \quad (46)$$

Deep in the gapped phase, we can expand $\cos(\sqrt{2\pi}\theta_-)$ around its minimum $\theta_- = \theta_{\rm min} + \delta\theta$. Integrating the massive $\delta\theta$ mode, the model for the charge field φ_+ maps to a Giamarchi-Schultz [33] model with Luttinger parameter $K' = 2K$. Therefore, the random disorder is a relevant perturbation for $K < 3/4$.

C. Conductance as a function of temperature

At energy scales above $\Delta_{\rm edge} \sim t_{\perp}e^{-\pi/2|\tilde{g}|}$, the conductance is dominated by the single-particle tunneling [20]. For the moderate interaction strength, this perturbation is irrelevant, and conductance increases upon lowering the temperature. Below the energy scale $\Delta_{\rm edge}$, two-particle processes are dominant, and they open the gap in the spin sector. In the topological phase ($g' < 0$), this gap protects the conducting mode (for the charge sector) in the presence of a single impurity, while in the topologically trivial phase ($g' > 0$) it does not. For random disorder, the topological phase remains conducting for $K > 3/4$. A schematic dependence of conductance on temperature is shown in Fig. 4.

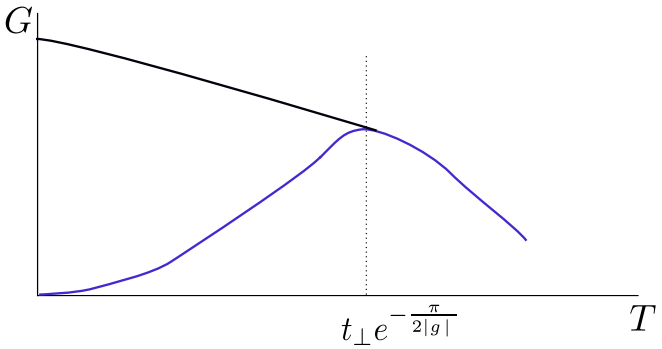

FIG. 4. Nonmonotonic conductance as a function of temperature for moderate interactions. At energies below the gap, $\Delta_{\rm edge} \sim t_{\perp}\exp(-\frac{\pi^2 u_-}{a_0|U-U_0|})$, the conductance renormalizes to zero in the presence of small concentration of impurities (blue curve) if $\tilde{g} = a_0(U_0 - U)/2\pi u_- > 0$ (spin-nematic phase). For $\tilde{g} = a_0(U_0 - U)/2\pi u_- < 0$ (spin-density-wave phase), the conductance remains finite (black curve). At energies above the gap, the conductance is dominated by single-particle tunneling.

D. Boundary zero modes in the protected phase

To reveal the existence of zero modes, we introduce a strong nonmagnetic impurity that pinches off a section of the helical modes. This discussion is then analogous to the one presented in [34,35] for the case of nonhelical chains. These impurities are modeled by

$$U_{\rm well} = ih_w\sum_{a,i}(R_a^{\dagger}L_{\bar{a}} + L_{\bar{a}}^{\dagger}R_a)\delta(x-x_i) + \text{H.c.} = \frac{2h_w}{\pi a_0}\cos(\sqrt{2\pi}\varphi_+)\cos(\sqrt{2\pi}\theta_-)\Big|_{x=0}^{x=L}, \quad (47)$$

where $x_1 = 0$ and $x_2 = L$, and δ is a Dirac delta function. The backscattering strength h_w is assumed to be larger than any other relevant energy scale in the problem. The potential well (47) pins the field θ_- to the value $\sqrt{\frac{\pi}{2}}m$ with $m \in \mathbb{Z}$, close to the boundary. In the bulk, the field θ_- is pinned to either $\sqrt{\frac{\pi}{2}}n$ for $g' > 0$ or $\sqrt{\frac{\pi}{2}}(n+1/2)$ for $g' < 0$. This implies that for $g' < 0$ the field θ_- has to change by $\pm\frac{1}{2}\sqrt{\frac{\pi}{2}}$ close to the boundary (see Fig. 5). This kink in the $\theta_-(x)$ field corresponds to a spin-1/4 excitation near the edge. The two different ground states correspond to configurations with kink and antikink pairs that are shown in Fig. 5. Both configurations have the same energy. This degeneracy of the θ_- field at the edge of the samples allows particles to tunnel in or out at the edges without paying the energy cost of the gap. One may therefore describe these modes as topologically protected localized zero mode at the boundaries of the sample [34,35].

As we discussed in the previous section, for $g' < 0$ the system is protected against localization by a single impurity due to the existence of the spin gap. Therefore, the spin-density-wave phase in this model is indeed topological, being protected against single-impurity backscattering and hosting

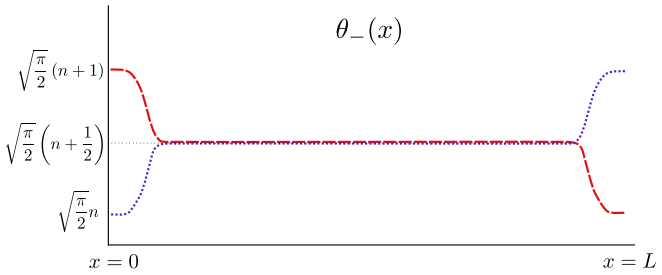

FIG. 5. Spatial profile of the $\theta_-(x)$ field in the topological phase ($g' < 0$). The two different ground states in a finite helical system correspond to the two choices of kink-antikink in the boundary, where the field has to minimize the backscattering potential. Different colors represent different ground-state profiles for $\theta_-(x)$.

fractionalized zero modes on its ends. By the same analysis, we find that the spin nematic phase is topologically trivial.

E. Experimental signatures

There are several predictions we have made that can be tested experimentally. First, the electric conductance studied above can be measured in a two-terminal experiment. In this measurement, one attaches Ohmic leads on the edge of the sample, as shown in Fig. 1. Our theory predicts the dependence of the two-terminal conductance on temperature; see Fig. 4.

Another type of experimental study involves a scanning tunneling microscope (STM). We propose to perform such an experiment after adding two nonmagnetic impurities to the system. Provided that the amplitude of the impurities is bigger than the size of the gap in bulk (Δ_{bulk}), a finite part of the helical mode is cut off from the rest of the system. If the system is in a topologically nontrivial phase, we expect to find fractional zero-energy modes at the end points of the constriction; see Fig. 6. By scanning the tip of the tunneling microscope away from the end points, one expected to see a hard gap in the density of states of the size Δ_{edge}. The tunneling density of

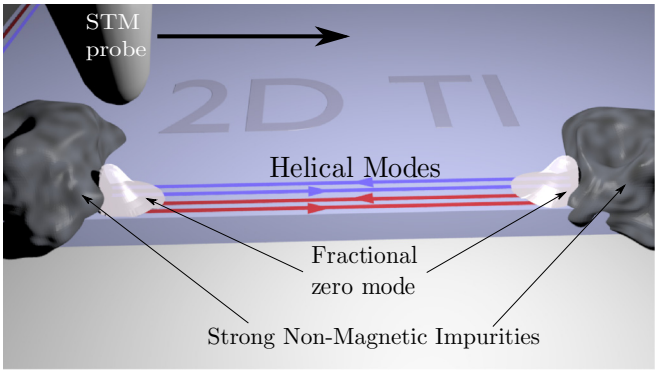

FIG. 6. Experimental setup for the detection of fractionalized zero modes. By moving the tip of STM parallel to the edge, one measures the tunneling current as a function of distance from the end point (see text).

TABLE I. Phases of two interacting helical modes. The interaction strength within the same helical state is U_0 and between different helical modes it is U.

	$U_0 > U$	$U_0 < U$
Topological protection	No	Yes
Order parameter	Spin nematic	Spin density wave
Zero modes	No	Yes

states in the topological phase scales as [31]

$$\frac{\nu(\epsilon)}{\nu_0} \propto \begin{cases} \left(\frac{\epsilon}{\Lambda}\right)^{\frac{1}{2K}-1}, & \text{close to the strong impurities,} \\ \theta(\epsilon - \Delta_{\text{edge}}), & \text{away from the impurities} \end{cases} \tag{48}$$

where ν_0 is a bare value of the density of states, ϵ is the energy of the tunneling electron with respect to the Fermi energy, and Λ is the ultraviolet cutoff. At low bias, the tunneling current has a power-law zero-bias anomaly near the end points (see Fig. 6), where the spin gap vanishes. Along the edge, but away from the impurities, the tunneling density of states $\nu(\epsilon)$ vanishes at bias smaller than Δ_{edge}.

V. CONCLUSIONS

In this paper, we studied the low-energy physics of two helical edge modes, coupled by tunneling and electron-electron interaction. Our results are summarized in Table I.

We showed that the tunneling between the modes, in the presence of repulsive interaction and generic spin-orbit interaction, leads to the development of a spin gap. If the interaction between Kramers partners is stronger than the interaction between states not connected by TR symmetry, the system is topologically trivial. The inclusion of weak nonmagnetic impurities localizes the conducting mode. The two-terminal conductance is a nonmonotonous function of temperature.

In the opposite limit, the system is in topologically nontrivial phase. The gap in the spin sector protects the conducting phase against backscattering by weak nonmagnetic impurities. The protected phase has a ground-state degeneracy and possesses fractionalized zero-energy edge modes. The latter can be observed in tunneling spectroscopy experiments. The two-terminal conductance monotonously grows with decreasing the temperature, reaching a value of $2e^2/h$ at zero temperature.

ACKNOWLEDGMENTS

The authors acknowledge discussion with Y. Gefen, N. Kainaris, A.D. Mirlin and E. Sela. This work has been supported by Israel Science Foundation (Grant No. 584/14), German Israeli Foundation (Grant No. 1167-165.14/2011).

[1] A. Kitaev, *Advances in Theoretical Physics: Landau Memorial Conference*, AIP Conf. Proc. No. 1134, edited by V. Lebedev and M. Feigel'man (AIP, New York, 2009), pp. 22–30.
[2] S. Ryu, A. P. Schnyder, A. Furusaki, and A. W. W. Ludwig, New J. Phys. **12**, 065010 (2010).
[3] C. L. Kane and E. J. Mele, Phys. Rev. Lett. **95**, 146802 (2005).
[4] B. A. Bernevig and S.-C. Zhang, Phys. Rev. Lett. **96**, 106802 (2006).
[5] M. König, S. Wiedmann, C. Brne, A. Roth, H. Buhmann, L. W. Molenkamp, X.-L. Qi, and S.-C. Zhang, Science **318**, 766 (2007).
[6] M. König, H. Buhmann, L. W. Molenkamp, T. Hughes, C.-X. Liu, X.-L. Qi, and S.-C. Zhang, J. Phys. Soc. Jpn. **77**, 031007 (2008).
[7] D. Hsieh, Y. Xia, L. Wray, D. Qian, A. Pal, J. H. Dil, J. Osterwalder, F. Meier, G. Bihlmayer, C. L. Kane, Y. S. Hor, R. J. Cava, and M. Z. Hasan, Science **323**, 919 (2009).
[8] D. Hsieh, D. Qian, L. Wray, Y. Xia, Y. S. Hor, R. J. Cava, and M. Z. Hasan, Nature (London) **452**, 970 (2008).
[9] Y. Xia, D. Qian, D. Hsieh, L. Wray, A. Pal, H. Lin, A. Bansil, D. Grauer, Y. S. Hor, R. J. Cava, and M. Z. Hasan, Nat. Phys. **5**, 398 (2009).
[10] D. Hsieh, Y. Xia, D. Qian, L. Wray, J. H. Dil, F. Meier, J. Osterwalder, L. Patthey, J. G. Checkelsky, N. P. Ong, A. V. Fedorov, H. Lin, A. Bansil, D. Grauer, Y. S. Hor, R. J. Cava, and M. Z. Hasan, Nature (London) **460**, 1101 (2009).
[11] P. Michetti, P. H. Penteado, J. C. Egues, and P. Recher, Semicond. Sci. Technol. **27**, 124007 (2012).
[12] B. Béri and N. R. Cooper, Phys. Rev. Lett. **108**, 206804 (2012).
[13] M. Levin and A. Stern, Phys. Rev. B **86**, 115131 (2012).
[14] E. Sela, A. Altland, and A. Rosch, Phys. Rev. B **84**, 085114 (2011).
[15] F. Crépin, J. C. Budich, F. Dolcini, P. Recher, and B. Trauzettel, Phys. Rev. B **86**, 121106(R) (2012).
[16] Y. Oreg, E. Sela, and A. Stern, Phys. Rev. B **89**, 115402 (2014).
[17] F. Geissler, F. Crépin, and B. Trauzettel, Phys. Rev. B **92**, 235108 (2015).
[18] T. L. Schmidt, S. Rachel, F. von Oppen, and L. I. Glazman, Phys. Rev. Lett. **108**, 156402 (2012).
[19] N. Kainaris, I. V. Gornyi, S. T. Carr, and A. D. Mirlin, Phys. Rev. B **90**, 075118 (2014).
[20] R. A. Santos and D. B. Gutman, Phys. Rev. B **92**, 075135 (2015).
[21] C. Wu, B. A. Bernevig, and S.-C. Zhang, Phys. Rev. Lett. **96**, 106401 (2006).
[22] Y. Tanaka and N. Nagaosa, Phys. Rev. Lett. **103**, 166403 (2009).
[23] C.-X. Liu, J. C. Budich, P. Recher, and B. Trauzettel, Phys. Rev. B **83**, 035407 (2011).
[24] A. A. Nersesyan, G. Japaridze, and I. Kimeridze, J. Phys.: Condens. Matter **3**, 3353 (1991).
[25] A. Gogolin, A. Nersesyan, and A. Tsvelik, *Bosonization and Strongly Correlated Systems* (Cambridge University Press, Cambridge, 2004).
[26] C. Wu, W. V. Liu, and E. Fradkin, Phys. Rev. B **68**, 115104 (2003).
[27] E. Fradkin, *Field Theories of Condensed Matter Physics* (Cambridge University Press, Cambridge, 2013).
[28] T. Giamarchi, *Quantum Physics in One Dimension*, International Series of Monographs on Physics (Clarendon, Oxford, 2003).
[29] A. Nersesyan, A. Luther, and F. Kusmartsev, Phys. Lett. A **176**, 363 (1993).
[30] S. T. Carr, B. N. Narozhny, and A. A. Nersesyan, Ann. Phys. (N.Y.) **339**, 22 (2013).
[31] O. Starykh, D. Maslov, W. Häusler, and L. Glazman, in *Interaction and Transport Properties of Lower Dimensional Systems*, Lecture Notes in Physics Vol. 544, edited by B. Kramer and T. Brandeis (Springer, Berlin, 2000).
[32] S. T. Carr, B. N. Narozhny, and A. A. Nersesyan, Phys. Rev. Lett. **106**, 126805 (2011).
[33] T. Giamarchi and H. J. Schulz, Phys. Rev. B **37**, 325 (1988).
[34] A. Keselman and E. Berg, Phys. Rev. B **91**, 235309 (2015).
[35] N. Kainaris and S. T. Carr, Phys. Rev. B **92**, 035139 (2015).